Immunity, Vol. 16, 803–814, June, 2002, Copyright ©2002 by Cell Press

Identification and Characterization of Thymic Epithelial Progenitor Cells

Andrea R. Bennett,[1,4] Alison Farley,[1] Natalie F. Blair,[1] Julie Gordon,[1] Linda Sharp,[2] and C. Clare Blackburn[1,3]

[1]Centre for Genome Research and Institute for Cell, Animal and Population Biology
The University of Edinburgh
King's Buildings
West Mains Road
Edinburgh EH9 3JQ

[2]Division of Biomedical and Clinical Laboratory Science
The University of Edinburgh
George Square
Edinburgh EH8 9XD
United Kingdom

Summary

T cell differentiation and repertoire selection depend critically on several distinct thymic epithelial cell types, whose lineage relationships are unclear. We have investigated these relationships via functional analysis of the epithelial populations within the thymic primordium. Here, we show that mAbs MTS20 and MTS24 identify a population of cells that, when purified and grafted ectopically, can differentiate into all known thymic epithelial cell types, attract lymphoid progenitors, and support $CD4^+$ and $CD8^+$ T cell development in *nude* mice. In contrast, other epithelial populations in the thymic primordium can fulfill none of these functions. These data establish that the $MTS20^+24^+$ population is sufficient to generate a functional thymus in vivo and thus argue strongly that all thymic epithelial cell types derive from a common progenitor cell.

Introduction

The unique processes of T cell differentiation and repertoire selection are mediated by specialized cellular microenvironments provided by the thymic stroma (Anderson et al., 1996; Miller, 1961; Anderson and Jenkinson, 2001). This comprises an ordered, three-dimensional network of epithelial cells interspersed with nonepithelial stromal cells and is broadly divided into two compartments, the cortex and the medulla, each of which contains several epithelial cell types (Boyd et al., 1993; Lampert and Ritter, 1988; van Ewijk et al., 1999). Interactions with multiple thymic epithelial cell types are required to support thymocyte maturation and selection. Thus, these cell types are functionally as well as phenotypically distinct (Anderson and Jenkinson, 2001; Ge and Chen, 2000; Lind et al., 2001). The lineage relationships between the thymic epithelial subpopulations and the molecular mechanisms underpinning their functional differences are, however, poorly understood.

Early thymus organogenesis, which occurs between day 9.5 and 11.5 of murine embryonic development (E9.5 and E11.5), results in the development from the third pharyngeal pouch of a common primordium containing prospective thymus and prospective parathyroid domains (Anderson and Jenkinson, 2001; Manley, 2000), delineated by expression of the transcription factors *Foxn1* and *Gcm2*, respectively (Gordon et al., 2001). The thymus and parathyroid primordia separate by E12.5, by which stage the thymic epithelial rudiment is encapsulated by mesenchyme. Mesenchyme-derived signals are required to support thymic development from E12.5 (Auerbach, 1960). Hematopoietic progenitors colonize the thymus from E11.5 (Itoi et al., 2001; Jotereau et al., 1987; Owen and Ritter, 1969), and during late organogenesis/patterning, reciprocal interactions between thymocytes and thymic epithelial cells are required to establish proper organization and function of the cortical and medullary compartments (Anderson and Jenkinson, 2001; Ritter and Boyd, 1993; van Ewijk et al., 1999). Vascularization may also be necessary for medullary maturation (Anderson et al., 2000) and may promote competence to support thymocyte maturation (Fairchild and Waldmann, 2000).

The precise embryonic origins of the thymus are controversial. In the predominant view, the cortical and medullary epithelia derive from the third pharyngeal cleft ectoderm and third pharyngeal pouch endoderm, respectively (e.g., Janeway and Travers, 1996; Parham, 2000), as suggested by histological analysis (Cordier and Haumont, 1980; Cordier and Heremans, 1975). However, neither a further histological study (Smith, 1965) nor elegant chick:quail chimera analyses (Le Douarin and Jotereau, 1975) found evidence for an ectodermal contribution but indicated a solely endodermal origin for the epithelial component of both compartments. Furthermore, a recent analysis, in which the medullary epithelium was shown to comprise largely clonal islets, challenges the proposal that one epithelial sheet generates the medulla and another the cortex (Rodewald et al., 2001).

Several marker studies also support a common origin for the cortical and medullary epithelia. mAb 4F1, which marks mature murine cortical epithelium, was reported to stain all thymic epithelial cells at E14 (Lampert and Ritter, 1988), and mAb A2B5, a marker of human thymic medulla, stained all epithelial cells in 7-week human fetal thymi (Haynes et al., 1984). Lampert and Ritter (1988) thus proposed that in early thymus organogenesis the entire epithelium coexpressed markers that later segregated to cortical or medullary epithelial cells and suggested the existence of a common precursor or stem cell for both cortical and medullary epithelial compartments. Consistent with this hypothesis, neoplastic human thymomas often expressed both cortical and medullary epithelial markers (Schleup et al., 1988), and "double-positive" cells were present in murine fetal thymic epithelial cultures (Ropke et al., 1995).

[3]Correspondence: c.blackburn@ed.ac.uk
[4]Present address: The Edward Jenner Institute for Vaccine Research, Compton, Newbury, Berkshire RG20 7NN, United Kingdom.

Recently, analysis of CD3ϵ26 mice, in which thymic epithelial development is arrested as a secondary effect of an early T cell development blockade, suggested that precursors for cortical epithelial cells may be characterized by a Keratin (K) 5^+8^+ phenotype (Klug et al., 1998). In adult wild-type mice, $K5^+K8^+$ cells constitute a minor population found at the cortico-medullary junction, while the major cortical and medullary subsets are $K8^+$ and $K5^+$, respectively (Klug et al., 1998). Thymi of adult CD3ϵ26 transgenic mice were predominantly $K5^+8^+$, but CD3ϵ26 thymi transplanted into $Rag1^{-/-}$ mice contained both $K5^+8^+$ and $K5^-8^+$ cells, suggesting a precursor:progeny relationship between these populations (Klug et al., 1998). The role of $K5^+K8^+$ cells in medullary epithelial development, however, was not addressed in this study (Klug et al., 1998), nor was the developmental potential of the $K5^+K8^+$ population analyzed directly. Notably, the expression patterns of K5 and K8 in normal thymus ontogeny have not been reported.

The *nu/nu* phenotype (*nude*) of congenital athymia is caused by mutation of the transcription factor, *Foxn1* (*whn/Hfh11*) (Kaestner et al., 2000; Nehls et al., 1994). Foxn1 is not required for initiation of thymus organogenesis (Nehls et al., 1996) but subsequently is required cell autonomously for the development of all major thymic epithelial subpopulations (Blackburn et al., 1996). In previous work, we analyzed the phenotype of cells apparently committed to thymic epithelial lineages, but unable to express Foxn1 (Blackburn et al., 1996), in *nude* mice and in *nude*:wild-type chimeras. Based on these analyses, we proposed that mAbs MTS20 and MTS24 identify progenitor cells for the entire thymic epithelium (Blackburn et al., 1996).

As MTS20 and MTS24 recognize extracellular determinants on the same epithelial cells (see Figure 2A), functional analysis of isolated $MTS20^+24^+$ cells is possible. We have therefore applied criteria predicted of thymic epithelial progenitor cells (TEPC) and their markers to $MTS20^+24^+$ cells within the murine thymic primordium. Furthermore, we have conducted an extensive phenotypic characterization of the E11.5 and E12.5 thymic primordia and of embryonic thymic $MTS20^+24^+$ cells. Our data establish that $MTS20^+24^+$ cells but not other epithelial cells within the E12.5 thymus primordium are specified progenitors capable of generating all thymic epithelial cell types and are sufficient to establish a functional thymus in vivo.

Results

Expression of the MTS20 and MTS24 Determinants Is Tightly Regulated during Thymus Ontogeny

We first analyzed the temporal expression of the MTS20 and MTS24 determinants, since TEPC markers should be enriched in the thymic primordium compared to later developmental stages. Thymus organogenesis commences at E9.5, and therefore we analyzed MTS20 and MTS24 expression in the pharyngeal arch region from this time point. From E9.5 to E11.5, flow cytometric analyses revealed small but highly consistent populations of $MTS20^+$ and $MTS24^+$ cells in the pharyngeal arch region (Figure 1A), and immunohistochemical analysis revealed strong staining with both markers in the prospective thymic primordium at E11.5 (Figure 1D). The fall in percentage of $MTS20^+$ and $MTS24^+$ cells at E11.5, as determined by flow cytometry, is likely due to the relative increase in volume of mesodermal/mesenchymal tissues ($MTS20^-$, $MTS24^-$), compared to endodermal tissues, that occurs between E10.5 and E11.5 in the pharyngeal region dissected for these analyses.

In thymi dissected from E12.5 embryos, flow cytometric analyses indicated MTS20 and MTS24 staining on approximately 35% of cells, which represented approximately 50% of epithelial cells in the E12.5 thymic primordium (Figures 1B and 1C). The MTS20 and MTS24 determinants were each strongly downregulated during subsequent thymus development, and only 1%–2% of cells were stained at E17.5 (Figures 1B and 1C); comparison of the percentage of $MTS20^+$ or $MTS24^+$ cells with that of cytokeratin$^+$ cells at each time point indicates that the proportion of epithelial cells expressing these antigens diminishes as organogenesis progresses (Figures 1B and 1C). In the adult thymus, MTS20 and MTS24 each recognize a rare subset of medullary epithelial cells (Godfrey et al., 1990; A.R.B., C.C.B., unpublished data).

Phenotypic Characterization of the Common Thymus/Parathyroid Primordium

The common thymus/parathyroid primordium forms from the third pharyngeal pouch between E10.5 and E11.5. Therefore, to determine the tissue restriction of the MTS20 and MTS24 determinants during thymus formation, we analyzed the spatial expression of MTS20 and MTS24 in the pharyngeal region at E11.5. Within this region, the MTS20 and MTS24 determinants were predominantly expressed throughout the common thymus/parathyroid primordium (Figure 1D), but some staining was also evident in endoderm adjacent to the primordium and in other endodermal derivatives (data not shown).

To relate our study to others addressing lineage relationships in the murine thymus, we also analyzed expression of K5 and K8 and of the 4F1 determinant in the pharyngeal region at E11.5, since the expression patterns of these markers in early thymus development are unreported. MTS10 staining, which identifies medullary epithelial cells in the adult thymus (Godfrey et al., 1990), was also analyzed.

At E11.5, K8 was strongly expressed throughout the common primordium and was expressed extensively in other epithelial structures, including the ectoderm and endoderm (Figure 1D, and data not shown). As expected, anti-K8 and anti-pan-cytokeratin staining was convergent in all tissues (data not shown). Within the common primordium, K5 expression was highly expressed in a smaller domain reminiscent of the prospective thymus domain identified by *Foxn1* expression (Gordon et al., 2001) (Figure 1D) and was expressed at lower levels in the prospective parathyroid domain; within this region, K5 and K8 colocalized in most, if not all, cells. K5 also stained ectoderm but was not highly expressed in the endoderm or other endodermal derivatives (data not shown).

4F1 staining was not apparent in the thymus/parathy-

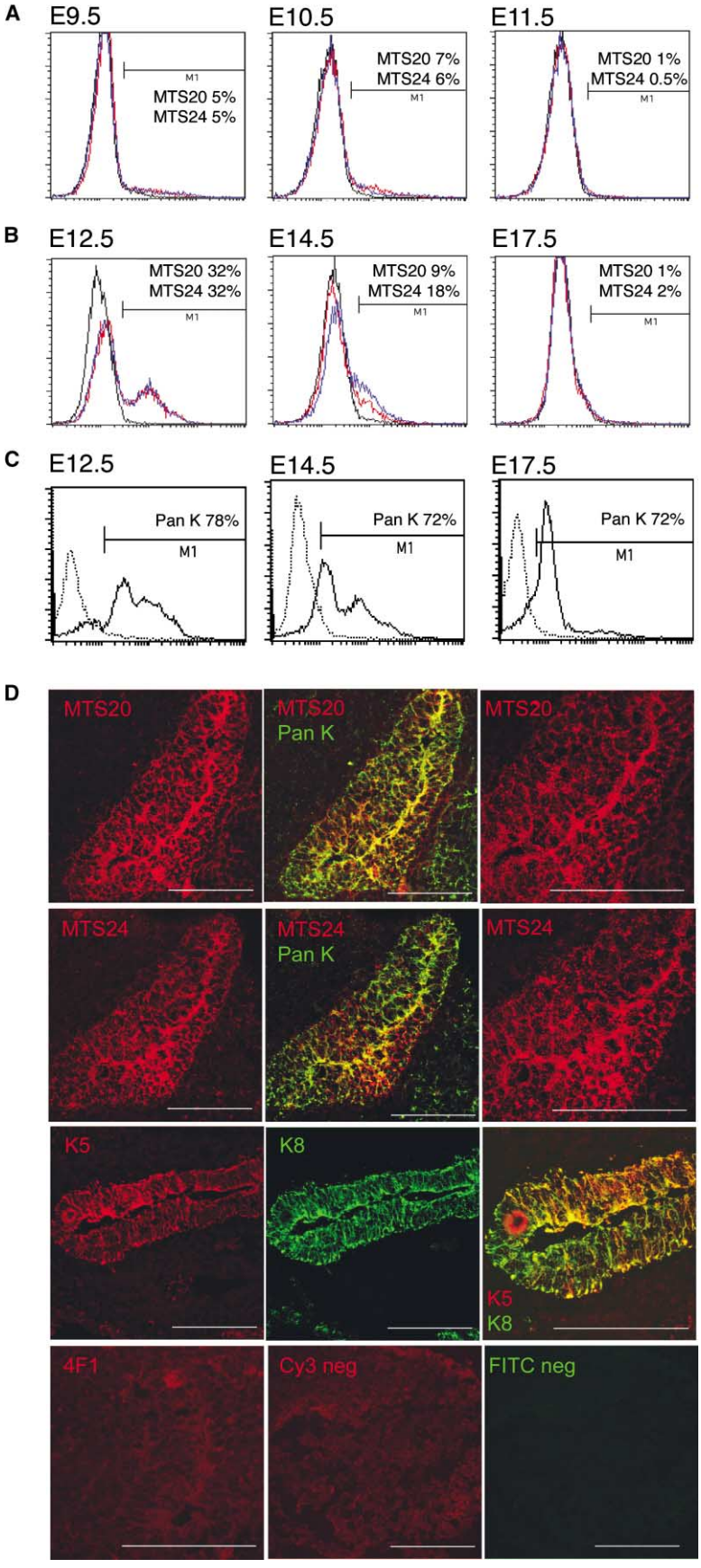

Figure 1. MTS20 and MTS24 Expression during Thymus Ontogeny

The second to fourth pharyngeal arch regions were dissected from E9.5 to E11.5 mouse embryos (A), or individual thymi were dissected from E12.5 to E17.5 embryos (B and C) and dissociated to single-cell suspensions or embedded for cryosectioning before staining. E17.5 thymi were depleted of $CD4^+$ and $CD8^+$ cells before flow cytometric analysis. (A) Flow cytometric analysis showing MTS20 and MTS24 staining in the second to fourth pharyngeal arch region (E9.5 to E11.5). (B) Flow cytometric analysis showing MTS20 and MTS24 staining in the developing thymus (E12.5 to E17.5). (C) Flow cytometric analysis showing pan-cytokeratin (Pan K) staining in the developing thymus (E12.5 to E17.5). (D) Immunohistochemical analysis showing MTS20, MTS24, K5, K8, Pan K, 4F1, and control (neg) staining in the common thymus/parathyroid primordium at E11.5. For (A) and (B), red line represents MTS20, blue line represents MTS24, black line represents isotype control. For (C), solid line represents anti-pan-cytokeratin; dotted line represents isotype control. (D) Scale bars, 100 μm. (A), (B), and (D) are representative of at least three separate experiments. (C) is representative of two experiments. For (A), mean ± SD (%): E9.5, MTS20, 5.2 ± 0.7, MTS24, 7.8 ± 3.7; E10.5, MTS20, 6.7 ± 0.6, MTS24, 7 ± 1; E11.5, MTS20, 1 ± 0.7, MTS24, 0.7 ± 0.8. For (B), mean ± SD (%): E12.5, MTS20, 34 ± 8.4%, MTS24, 35 ± 9.7%; E14.5, MTS20, 9 ± 1.2, MTS24, 17 ± 2.1; E17.5, MTS20, 1 ± 0.3, MTS24, 1.6 ± 0.1.

roid primordium (Figure 1D) but was seen in occasional cells scattered throughout the pharyngeal region (data not shown). We found no evidence of MTS10 staining at E11.5 (data not shown).

Collectively, these data are consistent with the existence of a common, MTS20$^+$24$^+$ thymic epithelial progenitor cell and suggest that such cells also express K5 and K8. However, functional analyses were required to address the precursor:product relationships suggested by this analysis directly.

MTS20 and MTS24 Identify a Discrete Population of Epithelial Cells within the Thymic Primordium

The E12.5 thymic primordium, the earliest stage at which the thymus can be manually dissected free of other tissues, is relatively enriched for MTS20$^+$24$^+$ cells compared to later stage thymi and was thus chosen as the source of cells for functional analyses. The cellular composition of the E12.5 thymus has not been reported in detail and was therefore analyzed prior to commencing functional studies.

In the E12.5 thymus, MTS20 and MTS24 were coexpressed by approximately 35% of cells (Figure 2A). No single-positive populations could be detected by flow cytometry, and therefore expression of these determinants appeared completely convergent at this developmental stage (Figure 2A). Immunohistochemical analysis revealed that MTS20$^+$24$^+$ cells were distributed throughout the primordium (Figure 2E), and foci of strongly staining cells were apparent. Both mAbs exhibited a distinctive, punctate staining pattern. The cells were epithelial, as evidenced by counterstaining with anti-pan-cytokeratin (Figure 2E).

The percentage of epithelial cells was determined by flow cytometry using anti-pan-cytokeratin, which bound approximately 75% of cells (Figure 2B). Notably, histological analysis indicated considerable size variation among E12.5 thymic epithelial cells (Figure 2E): this was also reflected in light scatter analysis of flow cytometric data (data not shown) and may explain the FACS profile obtained for cytokeratins at this and subsequent stages of development, which were characterized by two peaks of positive fluorescence.

Approximately 45% of E12.5 thymus cells expressed K8 (Figure 2C), and approximately 70% expressed K5 at varying levels (Figure 2C). The relative proportions of K5 and K8 cells varied somewhat between experiments, likely due to slight variations in the ages of the embryos and thus in the extent of differentiation within the organ. However, we consistently observed two K5$^+$ populations: most K5$^+$ cells coexpressed K8, while a smaller K5$^+$ population was K8$^-$ (Figure 2C). Similarly, double staining with anti-K8 and anti-pan-cytokeratin also revealed both double-positive and pan-cytokeratin single-positive populations (Figures 2C and 2E), indicating that not all E12.5 thymic epithelial cells express Keratin 8 at levels detectable by flow cytometry or immunofluorescence.

Immunohistochemical analyses were consistent with these findings. K5 was expressed at heterogeneous levels in the E12.5 primordium and colocalized with K8 in most cells (Figure 2E). Areas of strong K5 staining were found mainly in central regions of the primordium and sometimes contained K8$^-$ cells (Figure 2E; and as determined by analysis of single optical sections obtained by confocal microscopy, data not shown) suggesting that these areas might correspond to areas of prospective medullary epithelium. Consistent with this suggestion, these areas also contained MTS10$^+$ cells (Figure 2E); MTS10 staining often identified clusters of two to three cells in keeping with the observation that the medullary epithelial islets arise from a single progenitor cell (Rodewald et al., 2001). K5 staining appeared weaker in peripheral regions of the E12.5 thymus (Figure 2E); in some sections these cells appeared K8$^+$K5$^-$ (data not shown), suggesting the acquisition of a K8$^+$5$^-$ cortical epithelial phenotype.

4F1 labeled approximately 35% of cells in the E12.5 primordium (Figure 2D); MTS24$^+$ cells did not exhibit high levels of 4F1 staining but stained weakly with 4F1 in some preparations (Figure 2D). Although 4F1 is a marker of cortical thymic epithelial cells, in our hands it appeared to stain both epithelial cells and mesenchymal cells in preparations of dissected E12.5 thymi, since the proportion of 4F1$^+$ cells was higher when increased amounts of connective tissue were included in the dissected tissue (data not shown). In keeping with this, immunohistochemical analysis indicated that 4F1 staining did not discriminate between the epithelial component of the thymic primordium and surrounding mesenchymal cells (data not shown).

Flow cytometric analysis using anti-phospho-Histone H3 demonstrated that over 90% of cells in the E12.5 thymus were actively proliferating (Chou et al., 1990) (data not shown). Anti-c-kit staining (Matsuzaki et al., 1993) indicated that 6% of cells were hemato-lymphoid lineage (data not shown).

To integrate these data, we analyzed MTS10, K5, and K8 staining in purified MTS20$^+$24$^+$ and MTS20$^-$24$^-$ cells. Flow cytometric analysis of the purified cells indicated that the MTS20$^+$24$^+$ population also expressed both K5 and K8 (Figure 3A); K8 staining was heterogeneous, a small fraction ($\sim$2%) of MTS20$^+$24$^+$ cells stained only weakly with K8. In the MTS20$^-$24$^-$ fraction, approximately 80% of cells expressed K5, and approximately 10% expressed K8 (Figure 3B). Immunohistochemical analysis of cells frozen immediately after sorting confirmed that MTS20$^+$24$^+$ cells expressed cytokeratin and were negative for, or stained very weakly with, 4F1 and MTS10 (Figure 3C).

These data indicate that several distinct epithelial populations are present within the E12.5 thymic primordium. These include (1) MTS20$^+$24$^+$ cells, which express K5 and K8 (but do not express high levels of the differentiation antigens 4F1 and MTS10) and constitute approximately 45% of epithelial cells, and (2) MTS20$^-$24$^-$ epithelial cells, of which $\sim$80% express K5 and $\sim$10% express K8, and which include cells expressing the MTS10 and 4F1 determinants, suggesting the presence of cells differentiating into cortical and medullary thymic epithelial cell types.

MTS20$^+$24$^+$ Cells Give Rise to All Thymic Epithelial Cell Types

We therefore analyzed the lineage potential of these populations directly, to determine (1) whether, as pre-

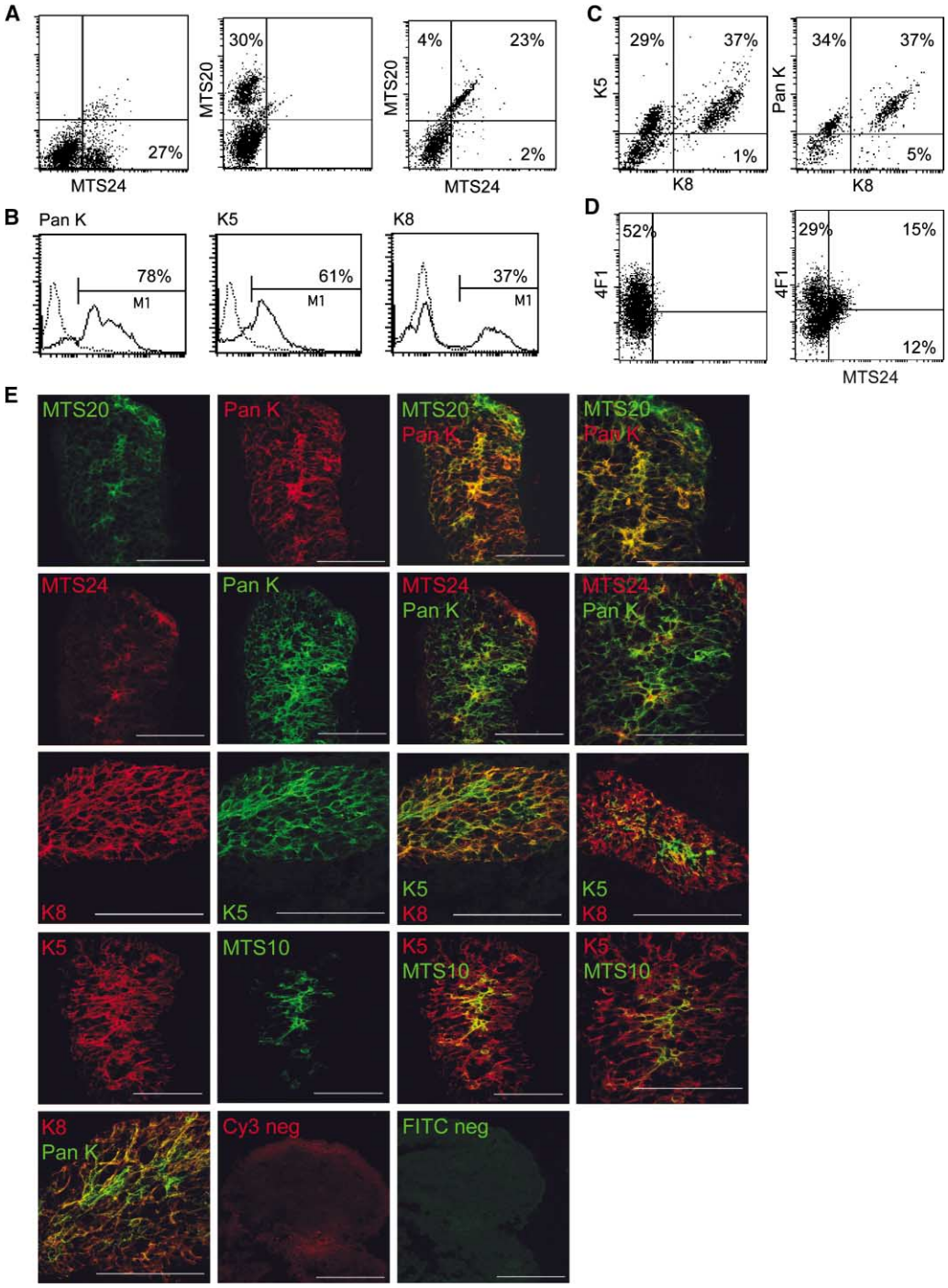

Figure 2. Cellular Composition of the Thymic Primordium

Thymi were dissected from E12.5 embryos and prepared as in Figure 1. (A) Left panel, staining with MTS24 and anti-rat IgG_{2a}-FITC. Center panel, staining with MTS20 and anti-rat IgM-PE. Right panel, double stain; MTS20 and MTS24 are coexpressed; no single-positive populations were detected. (B) Pan-cytokeratin (Pan K) is expressed by 78%, K5 by 61%, and K8 by 37% of thymus primordium cells. (C) Left panel, double stain with anti-K5 (PE) and anti-K8 (FITC) showing $K5^+8^+$ and $K5^+8^-$ populations. Right panel, double stain with anti-pan-cytokeratin (Pan K; PE) and anti-K8 (FITC) showing Pan K^+8^+ and Pan K^+8^- populations. (D) Left panel, 4F1 staining; right panel, double stain of 4F1 (PE) and MTS24 (FITC). (E) Fluorescence confocal microscopy analysis showing MTS20, MTS24, Pan K, K5, K8, MTS10, and isotype control staining (neg) in the E12.5 thymus primordium. (B) Dotted line represents isotype control, and solid line represents test antibody. (A and D) Dead cells were excluded by gating out 7-AAD positive cells. (B and C) Ungated samples shown. (E) Scale bars, 100 μm. (A)–(E) are representative of at least three separate experiments. For (A), mean ± SD: MTS20, 34 ± 8.4%; MTS24, 35 ± 9.7%. For (B), mean ± SD: pan K, 74.2 ± 20; K5, 68.5 ± 17; K8, 44.1 ± 5. For (D), mean ± SD: 4F1, 37 ± 6.7%.

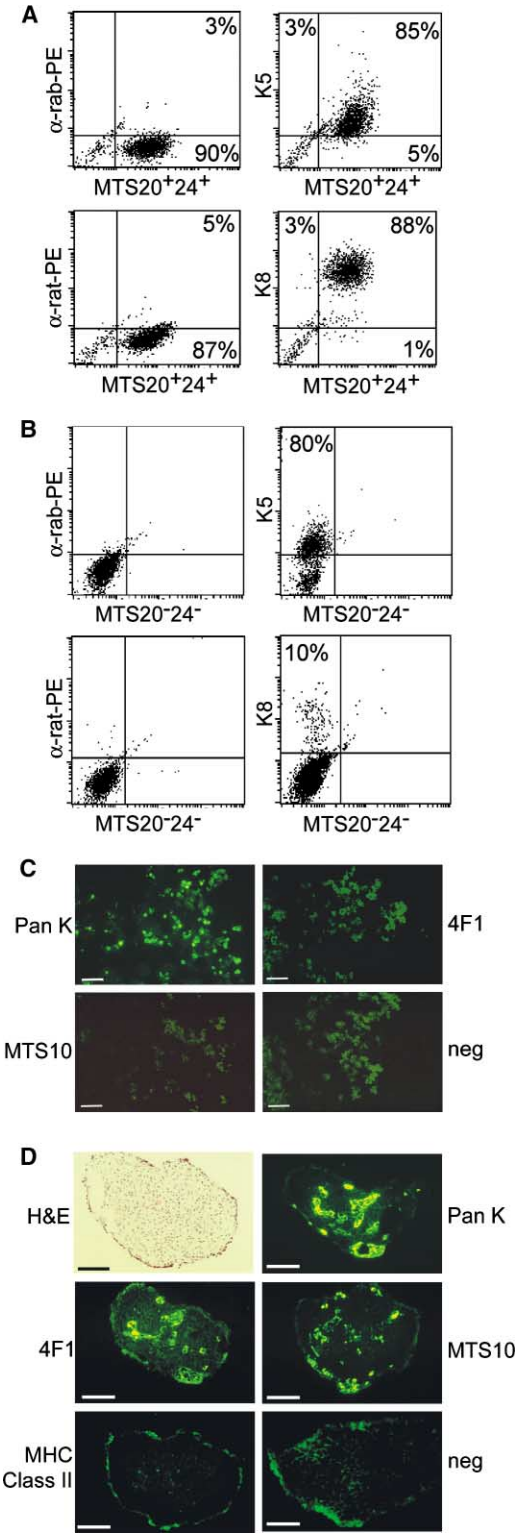

Figure 3. Characterization of Purified MTS20$^+$24$^+$ Cells

(A) MTS20$^+$24$^+$ cells were purified by flow cytometry, then stained for expression of K5 and K8. The MTS20$^+$24$^+$ population expresses both K5 and K8. (B) Purified MTS20$^-$24$^-$ cells were stained for expression of K5 and K8. K5 is expressed by 80% and K8 by 10% of MTS20$^-$24$^-$ cells. (C) MTS20$^+$24$^+$ cells were snap frozen immediately after purification and analyzed by immunohistochemistry using anti-pan-cytokeratin (Pan K), MTS10, 4F1, or secondary antibody only (neg). Panels show cytokeratin staining and lack of 4F1 or MTS10 staining in this population. (D) Purified E12.5 MTS20$^+$24$^+$ cells were aggregated for 48 hr in the presence of MEF, and then analyzed by immunohistochemistry using anti-pan-cytokeratin, anti-MHC class II, 4F1, and MTS10. Clusters of cells in each reaggregate were positive for pan-cytokeratin, 4F1, and MTS10 but remained negative for MHC class II. (A and B) Dead cells were excluded by gating. (A), (C), and (D) are representative of at least three experiments; (B) is representative of two experiments. (C and D) Scale bars, 100 μm.

dicted, TEPC-activity was present in the MTS20$^+$24$^+$K5$^+$8$^+$ population, (2) whether this population could generate both cortical and medullary compartments, (3) whether MTS20$^+$24$^+$K5$^+$8$^+$ cells were sufficient to establish a functional thymus, and (4) whether TEPC activity could be detected in other E12.5 thymus populations.

For these analyses, the thymic primordium was partitioned into two fractions, MTS20$^+$24$^+$ and MTS20$^-$24$^-$. The latter included the MTS20$^-$24$^-$K5$^+$MTS10$^+$ population, other epithelial cell types, and nonepithelial cells. Purities of greater than 98% for MTS20$^-$24$^-$ and greater than 95% for MTS20$^+$24$^+$ cells were routinely achieved, as determined by flow cytometric analysis of the sorted populations.

The lineage and functional potential of purified MTS20$^+$24$^+$ and MTS20$^-$24$^-$ cells was analyzed using a model based on reaggregate fetal thymic organ culture (Anderson et al., 1993). Here, defined numbers of purified cells and primary murine embryonic fibroblasts (MEF) were mixed, reaggregated for 24–48 hr in vitro, and then either analyzed directly or grafted under the kidney capsule of *nude* mice and left for 3–12 weeks before analysis. Importantly, since nude/Foxn1 is required cell autonomously for development of mature thymic epithelial cells (Blackburn et al., 1996), recipient cells were unable to contribute to any thymic epithelium generated in these experiments.

After 48 hr in culture, some cells in the MTS20$^+$24$^+$ cell reaggregates had gained a strongly 4F1$^+$ or MTS10$^+$ phenotype (Figure 3D), suggesting that differentiation had commenced; the level of 4F1 staining seen in these reaggregates was equivalent to that seen in mature thymic cortical epithelium (data not shown). Similar numbers of 4F1$^+$ and MTS10$^+$ cells were seen, which together constituted the majority of epithelial cells in each reaggregate as determined by anti-pan-cytokeratin staining (Figure 3D). Therefore, this staining was not attributable to contaminating 4F1$^+$ or MTS10$^+$ cells, which would constitute less than 2% of the epithelial cell content of the reaggregates based on sort purity. MHC class II expression could not be detected, indicating that the cells were still functionally immature at this time point (Figure 3D).

Three weeks after grafting, robust grafts were recovered from all MTS20$^+$24$^+$ cell-recipient mice (Figure 4A). These grafts were encapsulated and vascularized, and contained cells of lymphoid appearance (Figure 4B). Some grafts contained a central epithelium-lined cyst (Figure 4B). Immunohistochemical analysis revealed extensive networks of cytokeratin$^+$ epithelial cells within each graft (Figure 4C). These mostly expressed MHC

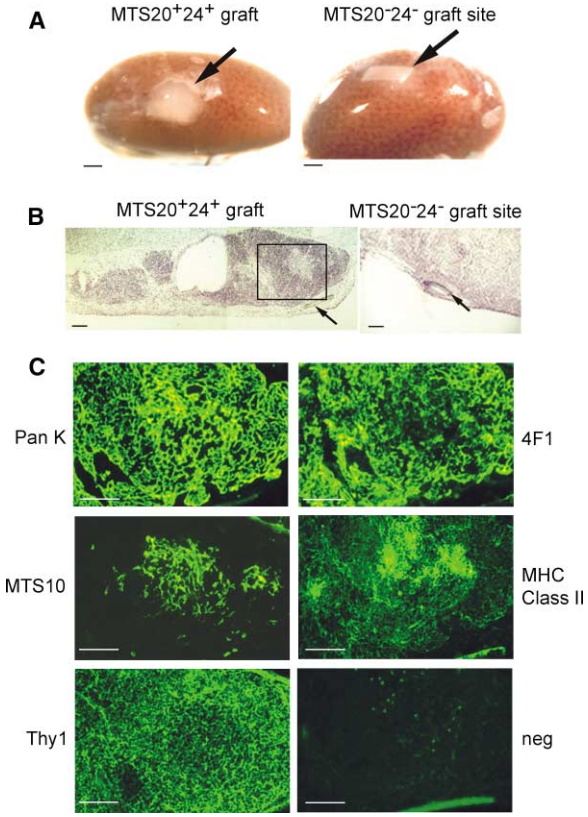

Figure 4. Analysis of Grafts Recovered from *nude* Mice

Thymic primordia were dissected from E12.5 embryos and partitioned into MTS20$^+$24$^+$ and MTS20$^-$24$^-$ fractions by flow cytometric sorting. Defined numbers of purified cells and primary embryonic fibroblasts were mixed, reaggregated for 24–48 hr in vitro, then grafted under the kidney capsule of *nude* mice, and left for 3 weeks before analysis. (A) MTS20$^+$24$^+$ cell graft, MTS20$^-$24$^-$ cell graft site. (B) Hematoxylin- and eosin-stained section of graft and graft site from (A). (C) MTS20$^+$24$^+$ cell graft stained for pan-cytokeratin (Pan K), 4F1, MTS10, MHC Class II, Thy-1, or secondary Ab only (neg). (A) Scale bars, 1 mm; (B and C) scale bars, 100 μm. Arrows in (A) and (B) point to graft site and to filter paper marking graft site. Box in (B) is area shown in (C). (A), (B), and (C) are representative of at least three experiments. Grafts contained 80,000, 12,500, and 12,500 (shown) MTS20$^+$24$^+$ cells, and 25,000, 12,500, and 12,500 (shown) MTS20$^-$24$^-$ cells.

class II (Figure 4C) and encompassed both 4F1$^+$ and MTS10$^+$ areas (Figure 4C). Indeed, medullary and cortical areas were clearly visible in hematoxylin- and eosin-stained sections (Figure 4B). K5 and K8 staining indicated the presence of all major thymic epithelial cell types identified by these markers (data not shown). The lymphoid cells within the grafts were Thy-1$^+$ (Van Ewijk et al., 1982) (Figure 4C) and B220$^-$ (data not shown), indicating that they were T lineage cells, and were found mainly within cytokeratin$^+$ areas. Some epithelial Thy-1 staining was also evident, in keeping with previous reports (Tucek and Boyd, 1990). Control grafts containing MEF alone survived in some recipients but were neither colonized by lymphoid cells nor expressed cytokeratin, 4F1, or MTS10 (data not shown). These data demonstrate that purified MTS20$^+$24$^+$ cells can differentiate into all currently identified populations of thymic epithelial cells and are able to form a vascularized thymus that attracts lymphoid precursors.

MTS20$^-$24$^-$ Cells Cannot Establish Thymi

We found no evidence of grafted cells in MTS20$^-$24$^-$ cell recipients (Figures 4A and 4B), although the graft sites were clearly marked in all animals. This was unexpected, since the MTS20$^-$24$^-$ population contained K5$^+$ (~80%) and K8$^+$ (~10%) epithelial cells and thus is likely to include cells differentiating into medullary and cortical epithelial cell types. Since the optimum growth and maturation of several thymic epithelial cell types is known to depend on appropriate interactions with thymocytes, a possible explanation for this was that MTS20$^-$24$^-$ cells required thymocyte-derived factors for growth/survival but were themselves unable to attract T cell progenitors. To test this possibility, we performed experiments in which MTS20$^+$24$^+$ and MTS20$^-$24$^-$ cell grafts were seeded with CD4$^-$8$^-$ thymocytes purified from adult thymi. Three weeks postgrafting, immunohistochemical analysis of MTS20$^+$24$^+$ grafts gave results identical to those described above; the grafts contained extensive networks of cytokeratin$^+$ epithelial cells which mostly expressed MHC class II (Figure 4C) and encompassed both 4F1$^+$ and MTS10$^+$ areas (data not shown). However, we were again unable to recover MTS20$^-$24$^-$ cell grafts (data not shown). Thus, purified MTS20$^-$24$^-$ cells could not establish thymus architecture or function even when supplied with immature thymocytes.

MTS20$^+$24$^+$ Cells Are Sufficient to Generate Functional Thymi in *nude* Mice

To test whether the MTS20$^+$24$^+$ cell-derived thymi were functionally as well as phenotypically mature, we analyzed thymocyte development in grafts seeded with CD4$^-$8$^-$ T cell progenitors. Flow cytometric analysis of thymocytes recovered from the MTS20$^+$24$^+$ cell grafts indicated that they had supported differentiation of CD4$^-$8$^-$ progenitors into CD4$^+$ and CD8$^+$ single-positive T cells; the distribution of the CD4$^+$ and CD8$^+$ subsets was identical to that within a normal adult thymus (Figure 5A). These data indicate the functional maturity of the differentiated epithelial cells within the MTS20$^+$24$^+$ grafts.

We also assayed the presence of peripheral T cells in recipient *nude* mice, since this provided a sensitive measure of gain of thymus function. In these experiments, MTS20$^+$24$^+$ or MTS20$^-$24$^-$ cell recipients were left for 12–16 weeks before analysis.

Significant CD4$^+$ and CD8$^+$ T cell populations were present in six out of seven MTS20$^+$24$^+$ cell-recipient mice (Figure 5B; Table 1). This included the four mice grafted with fewer than 500 MTS20$^+$24$^+$ cells. The mean numbers of T cells found in MTS20$^+$24$^+$ cell recipients were 9.2×10^5 CD4$^+$ and 6.6×10^5 CD8$^+$ cells (corrected for total lymph node cell number). Thus, the MTS20$^+$24$^+$-derived thymi had supported generation of total T cell numbers only 2-fold lower than those found in wild-type controls, in which an average of 2.1×10^6 CD4 and 1.4×10^6 CD8$^+$ T cells were found. These data indicate that MTS20$^+$24$^+$ cells are sufficient to generate a functional thymus and that fewer than 500 MTS20$^+$24$^+$ cells are required to confer thymus function on recipient mice.

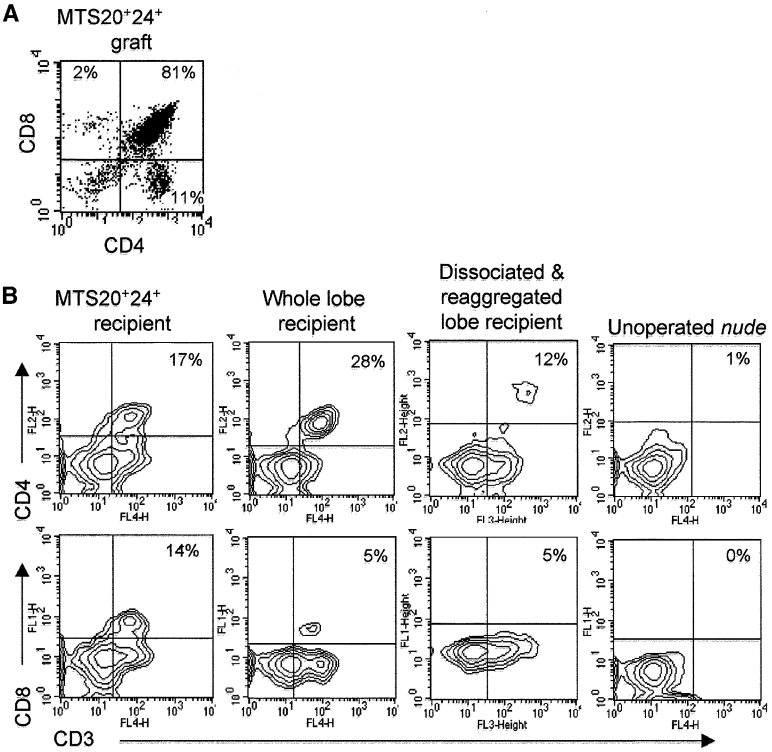

Figure 5. MTS20$^+$24$^+$ Cells Confer Thymus Function on *nude* Mice

Grafts were established as described in Figure 4 and left for 3 weeks (A) or 12–18 weeks (B) before analysis. For analysis, cells were recovered from the graft or pooled from the axillary, inguinal, and popliteal lymph nodes and analyzed for CD3, CD4, and CD8 expression. (A) Flow cytometric analysis of cells recovered from MTS20$^+$24$^+$ cell graft seeded with CD4$^-$8$^-$ thymocytes, showing development of CD4 and CD8 single- and double-positive populations. (B) CD4$^+$ and CD8$^+$ T cell populations in the lymph nodes of *nude* mice grafted with 500 MTS20$^+$24$^+$ cells or intact E12.5 thymus lobes. CD4$^+$ T cell population in the lymph nodes of *nude* mice grafted with 100,000 dissociated and reaggregated whole E12.5 thymus cells. No distinct T cell populations in lymph nodes from unmanipulated control *nude* mice. Figures refer to percentage of lymphoid cells in the upper right quadrant of each graph. MTS20$^+$24$^+$ cell grafts, n = 7; whole E12.5 thymus lobe grafts, n = 7; dissociated and reaggregated whole E12.5 thymus cell grafts, n = 9; unmanipulated mice, n = 15.

MTS20$^-$24$^-$ Cells Have No Thymus Generation Potential

Mice that received MTS20$^-$24$^-$ cells failed to gain thymus function (Table 1); a distinct T cell population was found in only one out of six recipients of MTS20$^-$24$^-$ cell grafts. The mean number of T cells present in MTS20$^-$24$^-$ cell recipients was 2.1 $\times$ 10^5 CD4$^+$ and 1.7 $\times$ 10^5 CD8$^+$ cells, indicating no increase in mean T cell numbers compared to ungrafted *nude* controls. Pooled lymph nodes from *nude* mice contained an average of 2.4 $\times$ 10^5 CD4$^+$ and 1.7 $\times$ 10^5 CD8$^+$ T cells. These data reinforced the short-term graft results, indicating that purified MTS20$^-$24$^-$ cells are unable to reconstitute any thymus functions.

Dissociated and Reaggregated E12.5 Thymus Cells Only Partially Generate Thymus Function

Unexpectedly, in control grafts provided by unfractionated, dissociated and reaggregated E12.5 thymus cells, only five out of nine grafted mice gained peripheral T cell populations. Significant CD8$^+$ T cell populations were not found in any dissociated and reaggregated cell recipients (Figure 5B; Table 1); in these mice, the pooled lymph nodes contained an average of 5.7 $\times$ 10^5 CD4$^+$ and 1.2 $\times$ 10^5 CD8$^+$ cells. This was surprising since these grafts contained equivalent cell numbers to grafts of two to twenty whole E12.5 thymus lobes. Thus, the potential of purified MTS20$^+$24$^+$ cells to establish thymus function was significantly greater than that of un-

Table 1. Analysis of Lymph Node Cells from Grafted *nude* Recipients

Graft	Graft Success[a]	Total LN Cells ($\times$10^6)	CD4$^+$ Cells per 10^3 LN Cells (SEM)	CD8$^+$ Cells per 10^3 LN Cells (SEM)
E12.5 MTS20$^+$24$^+$ cells	6/7[b]	20	46 (9.9)[d]	33 (9.1)[d]
E12.5 MTS20$^-$24$^-$ cells	1/6[c]	13	16 (7.2)[e]	13 (4.0)[e]
D&R E12.5 thymus cells	5/9	15	38 (10)[f]	7.8 (3.2)[f]
Intact thymus lobes (2)	7/7	19	190 (29)[g]	49 (14)[g]
MEF	0/3		11 (1)	7.7 (1)
Ungrafted *nude*	n = 15	24	10 (2.3)	7.4 (2)
Ungrafted wild-type	n = 12	8.8	240 (16)	160 (15)

[a] Grafts were taken to have conferred thymus function where T cell numbers in recipients exceeded two standard deviations from the mean of the ungrafted *nude* population.
[b] The unsuccessful graft contained 1 $\times$ 10^3 MTS20$^+$24$^+$ cells.
[c] The successful graft contained 1 $\times$ 10^4 MTS20$^-$24$^-$ cells.
[d] MTS20$^+$24$^+$ recipients versus ungrafted *nude*, p = 0.0006 for CD4$^+$, p = 0.011 for CD8$^+$.
[e] MTS20$^-$24$^-$ recipients versus ungrafted *nude*, p $>$ 0.6 for CD4$^+$, p $>$ 0.2 for CD8$^+$.
[f] Dissociated and reaggregated recipients versus ungrafted *nude*, p = 0.02 for CD4$^+$, p $>$ 0.4 for CD8$^+$.
[g] Whole lobe recipients versus ungrafted *nude*, p = 0.0002 for CD4$^+$, p = 0.010 for CD8$^+$.
Statistical significance was determined using the Mann-Whitney U Test; analyses include data from all mice in each group. SEM, standard error of the mean; D&R, dissociated and reaggregated; LN, lymph node.

fractionated, dissociated and reaggregated E12.5 thymus cells, particularly with respect to their potential to support $CD8^+$ T cell development.

Discussion

We have investigated lineage relationships within the thymic epithelium via phenotypic and functional analysis of cells expressing the MTS20 and MTS24 determinants, which we previously proposed as markers of TEPC (Blackburn et al., 1996). We have demonstrated that the MTS20 and MTS24 determinant expression profiles are consistent with those expected of TEPC markers and that, within the E12.5 thymic primordium, MTS20 and MTS24 are expressed by the same epithelial cells. We have further demonstrated that purified $MTS20^+24^+$ cells can differentiate into all known thymic epithelial subpopulations and that $MTS20^+24^+$ cells and/or their progeny can attract T cell progenitors and support T cell development. In contrast, $MTS20^-24^-$ cells can fulfill none of these functions, while unfractionated, dissociated and reaggregated E12.5 thymus cells show reduced thymus generation potential compared to $MTS20^+24^+$ cells. To our knowledge, these data constitute the first direct analysis of precursor:progeny relationships in thymus organogenesis. Taken together, they establish that within the E12.5 thymic primordium, full TEPC-potential is restricted to $MTS20^+24^+$ cells. Since $MTS20^+24^+$ cells could establish functional thymi when grafted ectopically, they further demonstrate that this population contains specified TEPC and is sufficient to establish a functional thymus in vivo.

Phenotype of TEPC

Previously, two laboratories had identified putative precursors for murine thymic epithelial cells; 4F1 was proposed to identify a common progenitor for cortical and medullary epithelium early in thymus development (Lampert and Ritter, 1988), and K5 and K8 were proposed to identify progenitors for at least cortical epithelial cells (Klug et al., 1998). We therefore related our findings to these data.

The $MTS20^+24^+$ population characterized herein binds 4F1 weakly but does not express the 4F1 determinant at the high levels characteristic of mature cortical thymic epithelium. In our hands, 4F1 expression is not detected in the E11.5 thymic primordium and does not discriminate between TEPC and other cell populations, including nonepithelial cells, in the E12.5 thymic rudiment. Therefore, from these data, 4F1 is not considered a useful TEPC marker.

K5 and K8 expression has not previously been described in early thymus ontogeny. Our analyses demonstrate that in both the E11.5 and E12.5 thymic primordium the major epithelial population is $K5^+8^+$, consistent with the hypothesis that cortical thymic epithelial precursor cells have a $K5^+8^+$ phenotype (Klug et al., 1998). We have also demonstrated that, at E12.5, the $MTS20^+24^+$ population coexpresses both K5 and K8. Thus, since $MTS20^+24^+$ cells can give rise to both cortical and medullary thymic epithelial lineages, we verify this hypothesis and further show that $MTS20^+24^+K5^+8^+$ cells are also precursors for medullary thymic cortical epithelium.

We are currently investigating the TEPC phenotype prior to E11.5. Notably, the MTS20 and MT24 determinants are expressed independently of *Foxn1* (Blackburn et al., 1996), suggesting that the phenotype of thymic epithelial founder cells in the murine embryo will be $MTS20^+24^+Foxn1^-$.

Full TEPC Potential Is Restricted to the $MTS20^+24^+$ Population

It is striking that $MTS20^-24^-$ cells generated no thymus functions in our assays, as the $MTS20^-24^-$ fraction contains $K5^+$, $K8^+$ cells, and $4F1^+$ cells and is therefore likely to include differentiating medullary and cortical thymic epithelial cells. As cortical epithelium has been believed to be sufficient to support T cell differentiation to the immature $CD4^+$ and $CD8^+$ single-positive stages (DeKoning et al., 1997; Ge and Chen, 2000), the inability of $MTS20^-24^-$ cells to form functional thymi suggests that, in addition to the roles described above, $MTS20^+24^+$ cells may be required to support the growth/survival of differentiating and/or mature cortical thymic epithelium. Furthermore, it demonstrates unequivocally that in the E12.5 thymus, full TEPC potential is restricted to the $MTS20^+24^+$ cell fraction.

It is formally possible that the $MTS20^+24^+K5^+8^+$ population contains distinct progenitors for the different mature thymic epithelial cell types. However, based on the present data, we suggest that a common progenitor gives rise to all thymic epithelial cell types and that, at E11.5 and E12.5, the phenotype of this progenitor is $MTS20^+24^+K5^+8^+$. Further work is required to determine the mechanisms via which $MTS20^+24^+$ cells generate the mature thymus; in particular, whether they differentiate directly into the different mature thymic epithelial cell types or whether they differentiate via compartment-specific intermediate progenitor cell populations, as recently suggested by analysis of medullary epithelial development (Rodewald et al., 2001).

Our data also demonstrate the increased potential of $MTS20^+24^+$ cells to generate thymus function compared to unfractionated, dissociated and reaggregated E12.5 thymus cells, particularly with respect to ability to support $CD8^+$ T cell development. This was unexpected since the cellular composition of the dissociated and reaggregated population is equivalent to an intact E12.5 thymic lobe. It is thus possible that in an inappropriate spatial context, $MTS20^-24^-$ E12.5 thymus cells have an inhibitory effect on the ability of $MTS20^+24^+$ cells to proliferate/differentiate or to orchestrate thymus organogenesis de novo. Alternatively, as the dissociated and reaggregated populations were not purified using mAbs, crosslinking of the MTS20 and/or MTS24 antigens may be responsible for the observed results, suggesting a functional role for the MTS20 and/or MTS24 antigens in thymus organogenesis. Further investigation of the mechanisms regulating the differentiation of $MTS20^+24^+$ cells during thymus organogenesis, including identification of the MTS20 and MTS24 antigens, will be required to discriminate between these possibilities.

The data presented herein suggest the possibility of deriving cell lines corresponding to multipotent TEPC. Such cell lines, or primary $MTS20^+24^+$ TEPC, will provide a robust model for the dissection of molecular

mechanisms involved in thymus organogenesis and thymic epithelial cell function. They would also present the possibilities of supporting T cell differentiation in vitro with a single epithelial cell line and of restoring thymic function to athymic individuals (Markert et al., 1999).

Concluding Remarks

We have presented a detailed analysis of the thymic primordium and have directly investigated the lineage potential of its constituent populations. These experiments demonstrate that, within the E12.5 thymus primordium, full TEPC potential is restricted to the MTS20$^+$24$^+$ population, which is sufficient to establish a thymus in vivo. Based on these data, we propose that a common MTS20$^+$24$^+$K5$^+$8$^+$ progenitor may give rise to all murine thymic epithelial cells. Further testing of this hypothesis will await the development of techniques suitable for clonal analysis of thymic epithelial progenitor cells.

Experimental Procedures

Antibodies

MTS20 (IgM) (Godfrey et al., 1990) and MTS24 (IgG$_{2a}$) (R.L. Boyd and D. Godfrey, unpublished data) are rat mAbs that recognize fixation-sensitive plasma membrane determinants and were a generous gift from Dr. R.L. Boyd, Monash University Medical Centre, Melbourne, Australia; 4F1 (IgM) (Imami et al., 1992) is a rat mAb that recognizes membrane and cytoplasmic determinants in cortical thymic epithelial cells and was a kind gift from Prof. M. Ritter, Imperial College, London; MTS10 (BD PharMingen) is a rat mAb that recognizes fixation-sensitive cytoplasmic determinants in medullary thymic epithelial cells; anti-pan-cytokeratin (rabbit polyclonal anti-Keratin, Dako Corporation); rabbit anti-Keratin 5 (Covance Research Products); rat anti-Keratin 8 (Troma 1; developed by P. Brulet and R. Kemler and obtained from the Developmental Studies Hybridoma Bank, The University of Iowa, IA); anti-MHC class II (M5114-biotin); anti-Thy-1 (T24); anti-CD4 (GK1.5, R-PE-conjugated); anti-CD3 (14S-2C11 Cy-chrome-conjugated); anti-CD8 (53-6.7, FITC-conjugated) (all BD PharMingen). Appropriate isotype-control antibodies (BD PharMingen) provided negative controls in all experiments. Unconjugated mAbs were detected using goat anti-rat FITC (Jackson Laboratories), mouse anti-rat IgG$_{2a}$-FITC (Serotec), goat anti-rabbit FITC (Sigma), goat anti-rat R-PE (Jackson Laboratories), donkey anti-rabbit-R-PE (Jackson Laboratories), mouse anti-rat IgM-PE (BD Pharmingen), donkey anti-rat-Cy3 (Jackson Laboratories), or goat anti-rabbit-Cy3 (Jackson Laboratories).

Mice

Female C57BL/6 and male CBA mice were caged together overnight. The morning of finding the vaginal plug was designated embryonic day 0.5 (E0.5). Female ICRF *nu/nu* mice were obtained from Harlan UK and kept in isolated ventilated cages under sterile conditions.

Histology and Immunohistochemistry

Tissues for sectioning were washed in PBS and embedded in OCT compound (Bayer Diagnostics). Eight micrometer frozen sections were cut onto Poly-l-lysine (Sigma) coated slides. Sections were fixed briefly in cold acetone. For immunohistochemical staining, sections were blocked in 10% normal serum and incubated with primary antibody for 1–2 hr followed by incubation with the appropriate secondary antibody. Staining was analyzed using a Vannox AHBT3 microscope and photographed (Figures 3, 4, and 5), or using a Leica TCSNT confocal microscope (Leica Microsystems GmbH, Heidelberg, Germany) and Leica TCSNT software (Figures 1C and 2E). The confocal images presented are either single optical sections or projected focus stacks of serial optical sections.

Flow Cytometry

Solid tissues were dissociated in 2 mg/ml hyaluronidase, 0.7 mg/ml collagenase, and 0.05 mg/ml DNase (all Sigma) for 10 min, and then in 0.025% trypsin for 10 min at 37°C to a single-cell suspension. Cells were released from lymph nodes and adult thymi by passage through a 70 μm pore size cell strainer (Falcon). Inclusion of a small proportion of parathyroid cells and connective tissue cells was unavoidable in flow cytometric analyses of E12.5 thymi. Cells were incubated with mAbs in PBS/10% FCS at 4°C for 20 min and washed in PBS/FCS. 7-AAD (BD Pharmingen) was included in some double-staining protocols to allow exclusion of dead cells. For intracellular staining, cells were treated with Fix and Perm (Caltag Laboratories). Cells were analyzed on a FACScan (Becton Dickinson) or FACSCalibur (Becton Dickinson), and data are presented using CellQuest software (Becton Dickinson). Figure 5B shows data obtained after gating for lymphoid cells. For sorting, cells were prepared as above and stained with MTS20 and MTS24 followed by anti-rat-FITC (Jackson Labs). Sorting was performed on a FACStar (Becton Dickinson) or on a MoFlo (Cytomation). MTS20$^+$24$^+$ and MTS20$^-$24$^-$ cells were collected, and aliquots of the sorted cells were reanalyzed on a FACScan (Becton Dickinson). In histograms showing flow cytometric analysis, percentages refer to marker region and have had background subtracted. Means and standard deviations refer to percentages of cells in marker region after subtraction of background and after gating out dead cells based on light scatter.

Cells

Murine embryonic fibroblasts (MEF) were prepared from E13.5 or E14.5 wild-type embryos stripped of their internal organs, including thymi, and triturated to a single-cell suspension. These cells were plated in DMEM (Gibco) containing 10% FCS, 50 U/ml penicillin, and 50 μg/ml streptomycin, and were harvested by trypsinization (0.025% trypsin) after a minimum of 3 days. Double-negative thymocytes were prepared by MACS depletion of CD4$^+$ and CD8$^+$ cells from thymocytes recovered from adult thymi, according to the manufacturer's instructions (Miltenyi Biotech). MTS20$^+$24$^+$ and MTS20$^-$24$^-$ cells were prepared from thymi dissected from early E12.5 embryos, as above. At E12.5 each thymic lobe contains approximately 5000 cells (A.R.B., C.C.B.). Thus, approximately 3500 MTS20$^+$24$^+$ cells and approximately 6500 MTS20$^-$24$^-$ cells constitute the equivalent number of cells of each population to that found in two intact E12.5 thymus lobes.

Kidney Capsule Grafting

Reaggregate cultures were prepared as described (Anderson et al., 1993). After 24–48 hr the reaggregate was grafted under the kidney capsule of female ICRF *nu/nu* mice with a small piece of filter paper to mark the position of the graft (Hoffmann et al., 1992). The grafting conditions used are listed below.

Short-Term Grafts

MTS20$^+$24$^+$ cell grafts: 12,500 cells (n = 2); 80,000 cells (n = 1). MTS20$^-$24$^-$ cell grafts: 12,500 cells (n = 2); 25,000 cells (n = 1). All with 100,000 MEF. All both with and without 100,000 CD4$^-$8$^-$ thymocytes.

Long-Term Grafts

MTS20$^+$24$^+$ cell grafts: 500 cells (n = 1); 500 cells plus 1000 MEF (n = 1); 500 cells plus 200,000 MEF (n = 2); 1000 cells plus 1000 MEF (n = 1); 1000 cells plus 200,000 MEF (n = 1); 5000 cells (n = 1). MTS20$^-$24$^-$ cell grafts: 500 cells plus 200,000 MEF (n = 2); 1000 cells plus 200,000 MEF (n = 1); 10,000 cells (n = 1); 10,000 cells plus 4000 MEF (n = 1); 160,000 cells plus 100,000 MEF (n = 1). Dissociated and reaggregated E12.5 thymus cell grafts: 10,000 cells (n = 6); 10,000 cells plus 1000 MEF (n = 2); 100,000 cells (n = 1). Unmanipulated *nu/nu* control mice were age matched and from the same purchase group in all experiments. Since loss of cells during experimental procedure is inevitable in this model, the input cell numbers cited are overestimated.

Acknowledgments

We thank R.L. Boyd, J. Gill, and M. Malin for generous provision of antibodies and discussion of unpublished data; T. Aebischer, C.L. Bennett, L. Colledge, A. Medvinsky, G. Morahan, C. Nowell, A.G.

Smith, and V.A. Wilson for critical discussion and comments on the manuscript; S. LeMoenic and A. Sanderson for flow cytometry; J. Nichols for technical advice; and Biomed Unit staff for animal care. This work was supported by The Wellcome Trust (A.R.B., C.C.B.), The Leukaemia Research Fund (C.C.B., A.F.), and The Medical Research Council (J.G.).

Received: October 29, 2001
Revised: April 24, 2002

References

Anderson, G., and Jenkinson, E. (2001). Lymphostromal interactions in thymus development and function. Nature Rev. Immunol. *1*, 31–40.

Anderson, G., Jenkinson, E.J., Moore, N.C., and Owen, J.J.T. (1993). MHC class II positive epithelium and mesenchyme cells are both required for T-cell development in the thymus. Nature *362*, 70–73.

Anderson, G., Moore, N.C., Owen, J.J.T., and Jenkinson, E.J. (1996). Cellular interactions in thymocyte development. Annu. Rev. Immunol. *14*, 73–99.

Anderson, M., Anderson, S.K., and Farr, A.G. (2000). Thymic vasculature: organizer of the medullary epithelial compartment? Int. Immunol. *12*, 1105–1110.

Auerbach, R. (1960). Morphogenetic interactions in the development of the mouse thymus gland. Dev. Biol. *2*, 271–284.

Blackburn, C.C., Augustine, C.L., Li, R., Harvey, R.P., Malin, M.A., Boyd, R.L., Miller, J.F.A.P., and Morahan, G. (1996). The *nu* gene acts cell-autonomously and is required for differentiation of thymic epithelial progenitors. Proc. Natl. Acad. Sci. USA *93*, 5742–5746.

Boyd, R.L., Tucek, C.L., Godfrey, D.I., Izon, D.J., Wilson, T.J., Davidson, N.J., Bean, A.G.D., Ladyman, H.M., Ritter, M.A., and Hugo, P. (1993). The thymic microenvironment. Immunol. Today *14*, 445–459.

Chou, M.Y., Chang, A.L.C., McBride, J., Donoff, B., Gallagher, G.T., and Wong, D.T.W. (1990). A rapid method to determine proliferation patterns of normal and malignant tissues by H3 mRNA in situ hybridization. Am. J. Pathol. *136*, 729–733.

Cordier, A.C., and Heremans, J.F. (1975). Nude mouse embryo: ectodermal nature of the primordial thymic defect. Scand. J. Immunol. *4*, 193–196.

Cordier, A.C., and Haumont, S.M. (1980). Development of thymus, parathyroids, and ultimo-branchial bodies in NMRI and nude mice. Am. J. Anat. *157*, 227–263.

DeKoning, J., DiMolfetto, L., Reilly, C., Wei, Q., Harvan, W.L., and Lo, D. (1997). Thymic cortical epithelium is sufficient for the development of mature T cells in relB-deficient mice. J. Immunol. *158*, 2558–2566.

Fairchild, P.J., and Waldmann, H. (2000). Extrathymic signals regulate the onset of T cell repertoire selection. Eur. J. Immunol. *30*, 1948–1956.

Ge, Q., and Chen, W.-F. (2000). Effect of murine thymic epithelial cell line (MTEC1) on the functional expression of $CD4^+CD8^-$ thymocytes subgroups. Int. Immunol. *12*, 1127–1133.

Godfrey, D.I., Izon, D.J., Tucek, C.L., Wilson, T.J., and Boyd, R.L. (1990). The phenotypic heterogeneity of mouse thymic stromal cells. Immunol. Today *70*, 66–74.

Gordon, J., Bennett, A.R., Blackburn, C.C., and Manley, N.R. (2001). *Gcm2* and *Foxn1* mark early parathyroid- and thymus-specific domains in the developing third pharyngeal pouch. Mech. Dev. *103*, 141–143.

Haynes, B.F., Scearce, R.M., Lobach, D.F., and Hensley, L.L. (1984). Phenotypic characterization and ontogeny of mesodermal derived and endocrine components of the human thymic microenvironment. J. Exp. Med. *159*, 1149–1168.

Hoffmann, M.W., Allison, J., and Miller, J.F.A.P. (1992). Tolerance induction by thymic medullary epithelium. Proc. Natl. Acad. Sci. USA *89*, 2526–2530.

Imami, N., Ladyman, H.M., Spanopoulou, E., and Ritter, M.A. (1992). A novel adhesion molecule in the murine thymic microenvironment: Functional and biochemical analysis. Dev. Immunol. *2*, 161–173.

Itoi, M., Kawamoto, H., Katsura, Y., and Amagai, T. (2001). Two distinct steps of immigration of haematopoietic progenitors into the early thymus anlage. Int. Immunol. *13*, 1203–1211.

Janeway, C.A.J., and Travers, P. (1996). Immunobiology, Second Edition (New York: Garland Publishing Inc.).

Jotereau, F., Heuze, F., Salomon-Vie, V., and Gascan, H. (1987). Cell kinetics in the fetal mouse thymus: precursor cell input, proliferation, and emigration. J. Immunol. *138*, 1026–1030.

Kaestner, K.H., Knochel, W., and Martinez, D.E. (2000). Unified nomenclature for the winged helix/forkhead transcription factors. Genes Dev. *14*, 142–146.

Klug, D.B., Carter, C., Crouch, E., Roop, D., Conti, C.J., and Richie, E.R. (1998). Interdependence of cortical thymic epithelial cell differentiation and T-lineage commitment. Proc. Natl. Acad. Sci. USA *95*, 11822–11827.

Lampert, I.A., and Ritter, M.A. (1988). The origin of the diverse epithelial cells of the thymus: is there a common stem cell? In Thymus Update, M.D. Kendall, and M.A. Ritter, eds. (London: Harwood Academic), pp. 5-25.

Le Douarin, N.M., and Jotereau, F.V. (1975). Tracing of cells of the avian thymus through embryonic life in interspecific chimeras. J. Exp. Med. *142*, 17–40.

Lind, E., Prockop, S.E., Porritt, H.E., and Petrie, H.T. (2001). Mapping precursor movement through the postnatal thymus reveals specific microenvironments supporting defined stages of early lymphoid development. J. Exp. Med. *194*, 127–134.

Manley, N.R. (2000). Thymus organogenesis and molecular mechanisms of thymic epithelial cell differentiation. Semin. Immunol. *12*, 421–428.

Markert, M.L., Boeck, A., Hale, L.P., Kloster, A.L., McLaughlin, T.M., Batchvarova, M.N., Douek, D.C., Koup, R.A., Kostyo, D.D., Ward, F.E., et al. (1999). Transplantation of thymus tissue in complete DiGeorge Syndrome. N. Engl. J. Med. *341*, 1180–1189.

Matsuzaki, Y., Gyotoku, J., Ogawa, M., Nishikawa, S., Katsura, Y., Gachelin, G., and Nakauchi, H. (1993). Characterization of c-kit positive intrathymic stem cells that are restricted to lymphoid differentiation. J. Exp. Med. *178*, 1283–1292.

Miller, J.F.A.P. (1961). Immunological function of the thymus. Lancet *2*, 748–749.

Nehls, M., Pfeifer, D., Schorpp, M., Hedrich, H., and Boehm, T. (1994). New member of the winged-helix protein family disrupted in mouse and rat nude mutations. Nature *372*, 103–106.

Nehls, M., Kyewski, B., Messerle, M., Waldschutz, R., Schuddekopf, K., Smith, A.J.H., and Boehm, T. (1996). Two genetically separable steps in the differentiation of thymic epithelium. Science *272*, 886–889.

Owen, J.J.T., and Ritter, M.A. (1969). Tissue interaction in the development of thymus lymphocytes. J. Exp. Med. *129*, 431–442.

Parham, P. (2000). The Immune System (New York: Garland Publishing).

Ritter, M.A., and Boyd, R.L. (1993). Development in the thymus: it takes two to tango. Immunol. Today *14*, 462–469.

Rodewald, H.R., Paul, S., Haller, C., Bluethmann, H., and Blum, C. (2001). Thymus medulla consisting of epithelial islets each derived from a single progenitor. Nature *414*, 763–768.

Ropke, C., van Soest, P., Platenburg, P.P., and van Ewijk, W. (1995). A common stem cell for murine cortical and medullary thymic epithelial cells? Dev. Immunol. *4*, 149–156.

Schleup, M., Willcox, N., Ritter, M.A., Newsom-Davis, J., Larchè, M., Janossy, G., and Howe, S. C. (1988). Myasthenia gravis thymus: clinical, histological and culture correlations. J Autoimmunity *1*, 445-467.

Smith, C. (1965). Studies on the thymus of the mammal. XIV. Histology and histochemistry of embryonic and early postnatal thymuses of C57BL/6 and AKR strain mice. Am. J. Anat. *116*, 611–630.

Tucek, C.L., and Boyd, R.L. (1990). Surface expression of CD4 and Thy-1 on mouse thymic stromal cells. Int. Immunol. *2*, 593–601.

Van Ewijk, W., Jenkinson, E.J., and Owen, J.J. (1982). Detection of Thy-1, T-200, Lyt-1 and Lyt-2-bearing cells in the developing lymphoid organs of the mouse embryo in vivo and in vitro. Eur. J. Immunol. *12*, 262–271.

Van Ewijk, W., Wang, B., Hollander, G., Kawamoto, H., Spanopoulou, E., Itoi, M., Amagai, T., Jiang, Y.F., Germeraad, W.T., Chen, W.F., and Katsura, Y. (1999). Thymic microenvironments, 3-D versus 2-D? Semin. Immunol. *11*, 57–64.